

# Exposing the dead-cone effect of jet quenching in QCD medium

---

Wei. Dai,<sup>a,1</sup> Ming-Ze Li,<sup>a</sup> Ben-Wei Zhang,<sup>b,c,1</sup> Enke Wang<sup>b,c</sup>

<sup>a</sup>*School of Mathematics and Physics, China University of Geosciences, Wuhan 430074, China*

<sup>b</sup>*Key Laboratory of Quark & Lepton Physics (MOE) and Institute of Particle Physics, Central China Normal University, Wuhan 430079, China*

<sup>c</sup>*Guangdong Provincial Key Laboratory of Nuclear Science, Institute of Quantum Matter, South China Normal University, Guangzhou 510006, China*

*E-mail:* [weidai@cug.edu.cn](mailto:weidai@cug.edu.cn), [bwzhang@mail.ccnucnu.edu.cn](mailto:bwzhang@mail.ccnucnu.edu.cn)

ABSTRACT: When an energetic parton traverses the hot QCD medium it may suffer multiple scattering and lose its energy. The medium-induced gluon radiation for a massive quark will be suppressed relative to that of a light quark due to the dead-cone effect. The development of new declustering techniques of jet evolution makes a direct study of the dead-cone effect in the QCD medium possible for the first time. In this work, we compute the emission angle distribution of the charm-quark initiated splittings in  $D^0$  meson tagged jet and that of the light parton initiated splittings in an inclusive jet in p+p and Pb+Pb at 5.02 TeV by utilizing the declustering techniques of jet evolution. The heavy quark propagation and induced energy loss in the QCD medium are simulated with the SHELL model based on the Langevin equation. When comparing the emission angle distribution of the charm-quark-initiated splittings and that of the light parton-initiated splittings by directly taking their ratios at the same energy intervals of the initial parton, the dead-cone effect in medium-induced radiation can be directly observed. We further investigate the case of the emission angle distributions normalized to the number of splittings and find the dead-cone effect will broaden the emission angle of the splitting and reduce the possibility to occur such splitting, therefore leading the massive parton to lose less energy.

---

<sup>1</sup>Corresponding author.

---

## Contents

<b>1</b>	<b>Introduction</b>	<b>1</b>
<b>2</b>	<b>Splitting-angle distributions in <math>D^0</math>-meson jets in p+p</b>	<b>2</b>
<b>3</b>	<b>Theoretical Framework of the in-medium Evolution of <math>D^0</math>-meson jets in A+A</b>	<b>4</b>
<b>4</b>	<b>Observation of the dead-cone in A+A collisions</b>	<b>6</b>
<b>5</b>	<b>Conclusions</b>	<b>9</b>

---

## 1 Introduction

In Quantum Chromodynamics (QCD), the vacuum is not transparent to a fast parton, and it induces gluon emissions in a process that can be described as a parton shower. The parton shower evolves into a multi-parton final state, then can hadronize into a cluster of final state hadrons in the same direction, which can be detected and recognized as jets [1]. It has been observed in particle colliders that the fast parton can be produced in the initial hard scatterings with large momentum transfer, and then make subsequent emissions resulting in additional productions of quarks and gluons, and then be reconstructed as jets in the final state.

One can expect the radiation from a parton of Mass ( $M$ ) and energy ( $E$ ) will be suppressed within an angular size of  $M/E$ . Such a phenomenon was named as the dead-cone effect [2], which manifested itself indirectly in various heavy flavor-related observables in particle collider experiments [3–6]. An iterative jet declustering technique [7–10] is emerged to help expose the jet substructure to the most basic splitting structure experimentally. ALICE report suggested a comparison between the emission angle distribution of charm-quark initiated splittings in  $D^0$ -meson tagged jets and that of light parton initiated splittings in inclusive jets produced in p+p collision at 13 TeV at proper radiator’s energy intervals. One can directly observe the dead-cone effect of the charm quark for the first time [11].

In high-energy nuclear-nuclear collisions, the fast parton produced in the initial hard scattering may pass through the de-confined state of quark and gluon plasma (QGP). The effect of its medium modification referred to as the jet quenching phenomenon [12–14] has been intensively studied theoretically and experimentally. The dominant mechanism of jet quenching is expected to be the radiation of soft gluons induced by the scattering of the fast parton with the medium constituents [15–24]. Such in-medium emission is also predicted to suffer the dead-cone effect which means the medium-induced radiation probability of the fast parton traversing the hot medium is also suppressed within an angular size of  $M/E$  [17, 25–27]. It may result in several observables which are explained by the scenario of the heavy

flavor quarks losing less energy than light flavor quarks in experimental measurements [28–32]. However, the dead-cone effect itself can not be isolated and observed through these measurements. In p+p collisions, iterative declustering techniques have allowed to expose the dead-cone effect. The application of such techniques to jets in heavy ion collisions might allow us to expose the dead-cone effect in medium-induced radiation and to understand the mass dependency of jet quenching. In this letter, we calculate the emission angle distribution of the charm-quark initiated in-medium splittings in  $D^0$ -meson tagged jets and that of the light parton initiated in-medium splittings in inclusive jets in Pb+Pb collisions at  $\sqrt{s} = 5.02$  TeV, and search to expose the dead-cone effect of medium-induced radiation in jet quenching.

## 2 Splitting-angle distributions in $D^0$ -meson jets in p+p

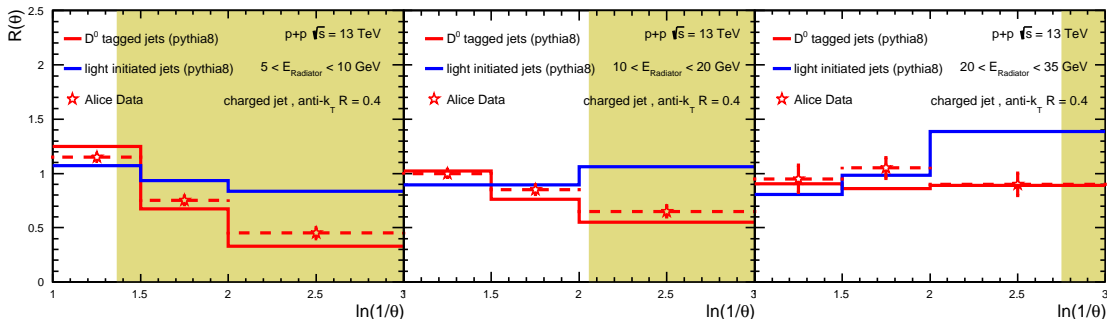


**Figure 1.** The ratios of the splitting-angle distributions for  $D^0$ -meson tagged jets (light-quark jets) to inclusive jets,  $R(\theta)$  in p+p collisions at  $\sqrt{s} = 13$  TeV using PYTHIA 8. The results are demonstrated for three energy intervals of the radiators:  $5 < E_{\text{Radiator}} < 10$  GeV (left panel),  $10 < E_{\text{Radiator}} < 20$  GeV (middle panel) and  $20 < E_{\text{Radiator}} < 35$  GeV (right panel) and they are compared with ALICE experimental data. The shaded areas correspond to the angles in which the radiation is suppressed due to the dead-cone effect, the mass of the charm quark is assumed to be  $1.275 \text{ GeV}/c^2$ .

By comparing the emission angle distribution of the heavy quark to that of the light flavor parton at the same initial energy in p+p collisions, the dead-cone effect can be observed. Such emission (splitting) processes should be extracted from jet substructures. The splitting-angle distributions of charm-quark initiated splittings in  $D^0$ -meson jets and the emission-angle distributions of light parton (gluon or light quark) initiated splittings in inclusive jets can be taken ratio to serve as an observable to reveal the dead-cone effect in vacuum radiation off a charm quark:

$$R(\theta) = \frac{1}{N^{\text{D}^0\text{jets}}} \frac{dn^{\text{D}^0\text{jets}}}{d\ln(1/\theta)} / \frac{1}{N^{\text{inclusive jet}}} \frac{dn^{\text{inclusive jet}}}{d\ln(1/\theta)} \quad (2.1)$$

where the  $\theta$  distributions are normalized to the number of jets for the same initial energy  $E_{\text{init}}$  intervals.  $N^{\text{D}^0\text{jets}}$  and  $N^{\text{inclusive jet}}$  denote as the numbers of jets for  $D^0$ -meson tagged jets and inclusive jets respectively. The ratios and the distributions are all expressed in terms of the inverse logarithm of the splitting angle,  $\ln(1/\theta)$ . If one assumes the

charm-quark to be massless, the no dead-cone limit of such observable can be derived from calculating the splitting-angle distribution in pure light-initiated jets from event generators and then replace the numerator in Eq. 2.1 to be  $(1/N^{\text{lightjets}})(dn^{\text{lightjets}}/d\ln(1/\theta))$ .

In order to verify the configurations and setups, and also to provide a p+p baseline for further investigation, we implement the same configurations of the event generator, methods, and analysis procedures as the experiment to calculate the observable of  $R(\theta)$ . PYTHIA 8 [33] and the anti- $k_T$  algorithm [34] from the Fastjet package [35] is used to simulate the production of the  $D^0$ -meson tagged jets with a transverse momentum in the interval of  $5 < p_{T,\text{jet}}^{\text{ch}} < 50$  GeV in p+p collisions, it requires that there should be only one  $D^0$ -meson candidate selected in the transverse-momentum interval  $2 < p_T^{D^0} < 36$  GeV/c. The Cambridge-Aachen (C/A) algorithm [36] is implemented to recluster the constituents in jets since it is also angular-ordered, the same as the QCD emissions. By iteratively declustering the splitting tree, the reclustering history and the measurements of the primary two prongs structures are recorded at each declustering step: the angle between the daughter prongs in splittings,  $\theta$ , the relative momentum transfer of the splitting,  $k_T$ , and the energy of the parton initiating the splitting (the radiator),  $E_{\text{Radiator}}$ .  $k_T > \Lambda_{\text{QCD}} = 200$  MeV/c is implemented to suppress the hadronisation effects [37]. And it should be noted that in each declustering step, the prongs containing  $D^0$ -meson candidates are always being followed. Splittings reconstructed from inclusive jets are then selected as references since the inclusive jets are dominated by massless gluon and nearly massless quark-initiated jets. However, there is no flavor tagging available in it. To be compatible with the splittings in  $D^0$ -meson jets, the leading prongs are consistently followed at each reclustering step and a minimum cut is imposed to the leading charged hadron in the leading prong of the recorded splitting in inclusive jets,  $p_{T,\text{inclusivejets}}^{\text{ch,leadinghadron}} \geq 2.8$  GeV/s which corresponds to the lower transverse momentum cut 2 GeV of the  $D^0$ -meson in  $D^0$ -meson jets.

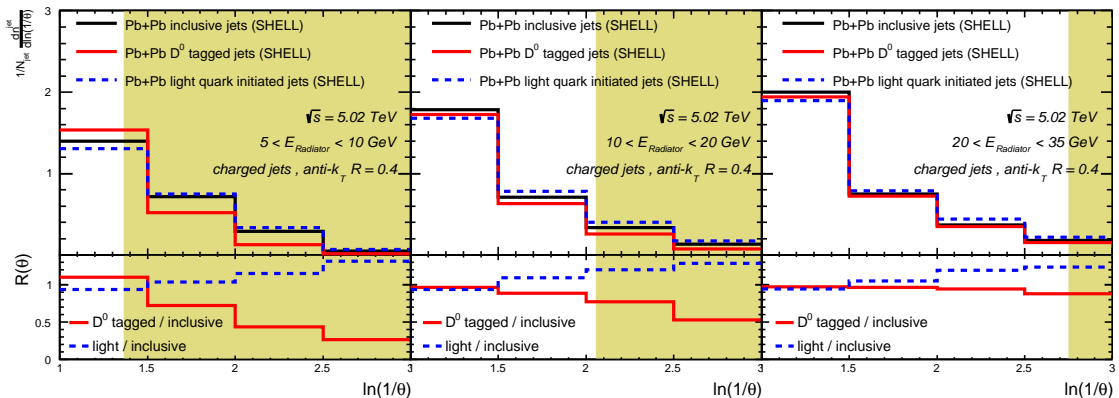


**Figure 2.** The splitting-angle distributions for  $D^0$ -meson tagged jets, inclusive jets and also light-quark jets normalized to the number of jets in Pb+Pb collisions at  $\sqrt{s} = 5.02$  TeV (upper plots) and also the  $D^0$ -meson tagged jets/inclusive jets (light-quark jets/inclusive jets) ratios (bottom plots) calculated for three energy intervals of the radiators:  $5 < E_{\text{Radiator}} < 10$  GeV (left panel),  $10 < E_{\text{Radiator}} < 20$  GeV (middle panel) and  $20 < E_{\text{Radiator}} < 30$  GeV (right panel). The shaded areas correspond to the angles at which the radiation is suppressed due to the dead-cone effect.

In Fig. 1, we reproduce the ratios of splitting-angle distributions  $R(\theta)$  for  $D^0$ -meson tagged jets (light-quark jets) to inclusive jets in p+p collisions at  $\sqrt{s} = 13$  TeV using PYTHIA 8. The results are demonstrated for three energy intervals of the radiators:  $5 < E_{\text{Radiator}} < 10$  GeV (left panel),  $10 < E_{\text{Radiator}} < 20$  GeV (middle panel) and  $20 < E_{\text{Radiator}} < 30$  GeV (right panel) which is as same as Ref. [11] in order to compare with ALICE data respectively. In these comparisons, PYTHIA 8 is proven to be sufficient to fairly describe the differences between the heavy and light quark initiated splitting angular distributions within a jet along with the analysis procedures mentioned above. The observable  $R(\theta)$  do can help demonstrate the differences of the radiation angular distributions of a charm quark and light quarks, then further expose the dead-cone effect of charm quark by illustrating suppression in the  $\ln(1/\theta)$  regions which are colored in each  $E_{\text{Radiator}}$  interval. These coloured areas are corresponding to the dead-cone angles in each intervals,  $\theta_{\text{dc}} < m_c/E_{\text{Radiator}}$ . With the increase of  $E_{\text{Radiator}}$ , we can observe the suppression in the lower  $\theta$  region is weaker due to the fact that the dead-cone region of  $\theta$  is smaller.

When understanding the ‘suppression,’ theoretically,  $R(\theta)$  can not compare with unity since  $N^{D^0\text{jets}}$  and  $N^{\text{inclusive jet}}$  will not be the same, the denominator of such ratio that is used to compare with the  $\theta$  distributions in  $D^0$ -meson tagged jets are reconstructed from inclusive jets in which there are light-quark, and gluon initiated splittings involved. Still, the advantage of such an observable is that it is experimentally measurable and still decisively manifests the suppression in the dead-cone region of  $\theta$ . Moreover, the plots with no dead-cone limits are also plotted accordingly. The deviations between the  $R(\theta)$  curve of  $D^0$ -meson tagged jets and the no dead-cone limit is much more pronouncing.

### 3 Theoretical Framework of the in-medium Evolution of $D^0$ -meson jets in A+A

When a fast parton traverses the hot medium, it will lose its energy by radiating gluons due to multiple scatterings within the medium, the radiative gluon spectrum is calculated from multiple gluon emission theories [15–24], in this letter, such spectrum is provided by the formalism from the Higher-Twist approach [15–17]:

$$\frac{dN}{dxdk_{\perp}^2 dt} = \frac{2\alpha_s C_s P(x)\hat{q}}{\pi k_{\perp}^4} \sin^2\left(\frac{t-t_i}{2\tau_f}\right) \left(\frac{k_{\perp}^2}{k_{\perp}^2 + x^2 M^2}\right)^4, \quad (3.1)$$

where  $x$  and  $k_{\perp}$  are the energy fraction and transverse momentum of a radiated gluon,  $M$  is the mass of the parent parton,  $\alpha_s$  is the strong coupling constant,  $C_s$  is the quadratic Casimir in color representation,  $P(x)$  is the vacuum splitting function [38], the jet transport coefficient  $\hat{q} \propto \hat{q}_0(T/T_0)^3$  [19],  $\tau_f = 2Ex(1-x)/(k_{\perp}^2 + x^2 M^2)$  is the gluon formation time.

The dead-cone effect manifests itself in the last quadruplicate term of Eq. (3.1). One can easily rewrite such term to be:  $(1 + \theta_0^2/\theta^2)^{-4}$  with the relation  $\theta_0 = M/E$  and  $k_{\perp} = xE\theta$ , the radiative gluon spectrum for massive quarks will be largely suppressed when the radiation angle  $\theta < \theta_0$ . It is very interesting to investigate how the detailed effect manifests itself in the QCD medium-modified emission angle distributions of heavy quark-initiated splittings.

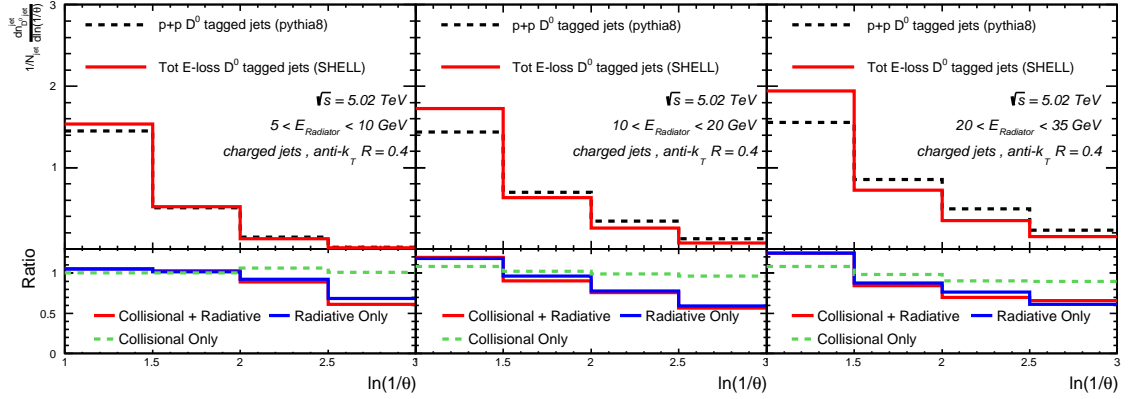


**Figure 3.** The splitting-angle distributions of the  $D^0$  meson tagged jets normalized to the number of jets in p+p and A+A collisions at  $\sqrt{s} = 5.02$  TeV (upper plots) and also their A+A/p+p ratios (bottom plots) calculated for three energy intervals of the radiators:  $5 < E_{\text{Radiator}} < 10$  GeV (left panel),  $10 < E_{\text{Radiator}} < 20$  GeV (middle panel) and  $20 < E_{\text{Radiator}} < 30$  GeV (right panel). Also the contributions from the radiative and collisional energy losses in A+A collisions are presented accordingly.

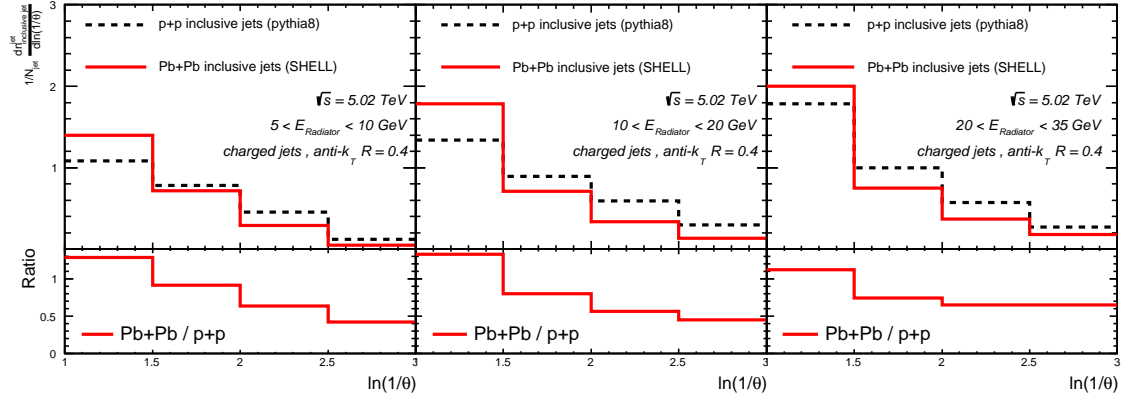


**Figure 4.** The splitting-angle distributions of the inclusive jets normalized to the number of jets in p+p (dash lines) and A+A (solid lines) collisions at  $\sqrt{s} = 5.02$  TeV (upper plots) and also their A+A/p+p ratios (bottom plots) calculated for three energy intervals of the radiators:  $5 < E_{\text{Radiator}} < 10$  GeV (middle panel),  $10 < E_{\text{Radiator}} < 20$  GeV (right panel) and  $20 < E_{\text{Radiator}} < 30$  GeV (left panel)

Taking advantage of the previous study in p+p collisions, we compute the same charm quark-initiated splittings and light parton-initiated splittings to demonstrate the possible dead-cone effect in A+A collisions. The Simulating Heavy quark Energy Loss with Langevin equations (SHELL) model [39–42] is employed to describe the in-medium evolution of the heavy and light parton considering both collisional and elastic energy loss mechanism. The SHELL model has already been utilized to predict the number of heavy flavor jet-related observable [3, 32, 43]. It is built on the framework of the modified Langevin equations describing the propagation of heavy quarks [39, 41, 42, 44, 45],

$$\Delta\vec{x}(t) = \frac{\vec{p}(t)}{E}\Delta t, \quad (3.2)$$

$$\Delta\vec{p}(t) = -\Gamma(p, T)\vec{p}\Delta t + \vec{\xi}(t)\sqrt{\Delta t} - \vec{p}_g(t), \quad (3.3)$$

where  $\Delta t$  is the time interval between each Monte Carlo simulation step, drag coefficient  $\Gamma$  is constrained by the fluctuation-dissipation relation [46] with momentum diffusion coefficient  $\kappa, \Gamma = \kappa/2ET = T/D_s E$  and  $D_s = 4/2\pi T$ .  $D_s$  is the spacial diffusion coefficient. The thermal stochastic term  $\vec{\xi}(t)$ , which is random kicks on the heavy quarks from thermal quasi-particles in QGP, obeys the Gaussian distribution  $\langle \xi^i(t)\xi^j(t') \rangle = \kappa\delta^{ij}\delta(t-t')$ . The last term in Eq. (3.3) is the momentum recoil due to the medium-induced gluon radiation, which is implemented with the higher-twist approach mentioned in Eq. 3.1. During each time interval, the in-medium gluon radiation probability, which is also calculated from Eq. 3.1 and assumed to obey the Poisson distribution, is implemented to decide whether radiation happens during a Langevin evolution time interval,  $P(n) = \lambda^n e^{-\lambda}/n!$  means the probability  $P(n)$  of radiating  $n$  gluons during such time interval  $\Delta t$ .  $\lambda$  is the mean value of  $n$  and can be calculated by integrating Eq. (3.1),

$$\lambda(t, \Delta t) = \Delta t \int dx dk_{\perp}^2 \frac{dN}{dx dk_{\perp}^2 dt} \quad (3.4)$$

If radiation occurs, the number of radiated gluons is determined by  $P(n)$  and the four-momentum of each radiated gluon can be updated in Eq. (3.1), *i.e.*, the last term  $\vec{p}_g$  of Eq. (3.3) in each time interval  $\Delta t$ . The simulation of a parton propagating in the hot and dense medium will keep evolving as described above until the temperature of the medium decreases to  $T_c = 165$  MeV. The space-time evolution of the QCD medium is provided by a (3+1)D viscous hydrodynamic model CLVisc [47]. An energy cutoff  $\omega_0 \geq \mu_D = \sqrt{4\pi\alpha_s}T$  is set to maintain the fluctuation-dissipation relation for heavy quarks, and the initial parton positions are provided by Glauber Monte Carlo [48]. The value of  $\hat{q}_0 = 1.5$  GeV<sup>2</sup>/fm is extracted from  $\chi^2$  calculations in final-state hadron productions in Pb + Pb collisions at  $\sqrt{s} = 5.02$  TeV [49, 50]. The value  $D_s(2\pi T) = 4$  extracted from  $\chi^2$  calculations in  $D$  meson  $R_{AA}$  between theoretical calculations and experimental data [51–54] is consistent with  $D_s(2\pi T) = 3.7 \sim 7$  obtained from Lattice QCD calculations [55, 56].

#### 4 Observation of the dead-cone in A+A collisions

In Fig. 2, the number of jets normalized splitting-angle distributions of charm-quark initiated splittings for D<sup>0</sup>-meson tagged jets and light parton initiated splittings for inclusive



jets are calculated in Pb+Pb collisions at  $\sqrt{s} = 5.02$  TeV displayed in the upper panels denoted as solid lines in different colors respectively. Then the ratio of these two distributions, which potentially can be served as an observable  $R^{AA}(\theta)$ , is expected to help expose the possible suppression in the dead-cone region of splitting-angle  $\theta$ . It is exactly what we observed in Fig. 2 in which the ratios are taken in the bottom panels; similar suppression at the  $\theta_{dc} < m_c/E_{\text{Radiator}}$  regions as in the case of p+p is observed. The no-quark mass (dead-cone) limit is also plotted as a reference. By comparing the  $R^{AA}(\theta)$  distributions as functions of  $\ln(1/\theta)$  with the no quark mass (dead-cone) limit at the different radiators' energy intervals, we find such suppression begins to vanish when the energy of the radiator increases. However, there will also be a mass effect in the collisional energy loss mechanism which is not expected to be affected by such suppression in the dead-cone region of the splitting angle. It is important to investigate such pollution to isolate the observation of the dead-cone effect implemented in the radiative energy loss mechanism.

To verify such suppression is truly due to the dead-cone effect embedded in the formalism of the higher-twist approach that describes the radiative energy loss due to multiple scattering, we compute in the upper panels of Fig. 3 the splitting-angle distributions of the  $D^0$  meson tagged jets normalized to the number of jets in Pb+Pb collisions at  $\sqrt{s} = 5.02$  TeV. Also, the A+A/p+p ratios from separate contributions for collisional energy loss and radiative energy loss in the bottom panel are denoted as the dashed line and solid lines respectively. We find that the radiative energy loss contribution would lead the distribution in Pb+Pb to shift to a larger  $\theta$  region than p+p for all three energy intervals of radiators. However, the collisional energy loss contribution would barely affect the  $\ln(1/\theta)$  distributions for the  $D^0$  meson-tagged jets in p+p. We can conclude that the collisional energy loss mechanism has a negligible impact on the medium modification to the emission angle distribution of the charm-quark initiated splittings for  $D^0$  meson-tagged jets. Only the radiative energy loss contribution will be responsible for the medium modification to the  $\ln(1/\theta)$  distributions for the  $D^0$  meson-tagged jets. Therefore,  $R^{AA}(\theta)$  can be computed using the same iterative jet declustering techniques applied in p+p and then measured experimentally, also it can be proposed to disclose the measurement of the dead-cone effect medium-induced radiation in jet quenching and further constrain the radiative energy loss description of jet quenching models and gain more understanding of the in-medium evolution of the jet shower.

We systematically investigate the medium modifications of the number of jets normalized emission angle distributions of the charm-quark (light parton) initiated splittings which are used to calculate  $R(\theta)$ , and also the mass dependencies of the emission angle distributions both in p+p and A+A by comparing the heavy and light case at the same energy intervals of the radiator. The averaged splitting angles per jets are calculated in  $D^0$ -meson (inclusive) jets in p+p and Pb+Pb at  $\sqrt{s} = 5.02$  TeV demonstrated in Table. 1 for each energy interval. Observing Fig. 3 and Fig. 4, we find the splitting-angle distributions are always shifting to larger  $\theta$  (small  $\ln(1/\theta)$ ) due to jet quenching; it is consistent with the values of the averaged splitting angles per jets in A+A are larger than their counterparts in p+p. From the observation in Fig. 1, we find the number of jets normalized emission-angle distribution ratios of the charm-quark and light parton in p+p is larger than



$E_{\text{Radiator}}$	Inclusive jets	$D^0$ jets	
	$\langle\theta\rangle_{\text{jets}}$	$\langle\theta\rangle_{\text{jets}}$	
5 – 10 GeV	0.31	0.34	pp
	0.36	0.36	AA
10 – 20 GeV	0.40	0.37	pp
	0.45	0.42	AA
20 – 35 GeV	0.47	0.42	pp
	0.49	0.47	AA

**Table 1.** The averaged splitting-angles in jets for  $D^0$ -meson tagged and inclusive jets are calculated in both p+p and Pb+Pb collisions at  $\sqrt{s} = 5.02$  TeV at three energy intervals:  $5 < E_{\text{Radiator}} < 10$  GeV,  $10 < E_{\text{Radiator}} < 20$  GeV and  $20 < E_{\text{Radiator}} < 30$  GeV respectively.

$E_{\text{Radiator}}$	Inclusive jets		$D^0$ jets		
	$\langle\theta\rangle_{\text{spl}}$	$N_{\text{spl}}$	$\langle\theta\rangle_{\text{spl}}$	$N_{\text{spl}}$	
5 – 10 GeV	0.227	1.358	0.277	1.233	pp
	0.256	1.405	0.280	1.280	AA
10 – 20 GeV	0.220	1.810	0.244	1.510	pp
	0.254	1.757	0.263	1.600	AA
20 – 35 GeV	0.232	2.040	0.232	1.822	pp
	0.249	1.977	0.251	1.860	AA

**Table 2.** The averaged splitting-angles per splitting for  $D^0$ -meson tagged and for inclusive jets are calculated in both p+p and Pb+Pb collisions at  $\sqrt{s} = 5.02$  TeV at three energy intervals:  $5 < E_{\text{Radiator}} < 10$  GeV,  $10 < E_{\text{Radiator}} < 20$  GeV and  $20 < E_{\text{Radiator}} < 30$  GeV. The numbers of splittings in jets are also provided accordingly.

1 at larger  $\theta$  and smaller than 1 at smaller  $\theta$  at the three energy intervals, but in the case in A+A demonstrated in Fig. 2, the ratios are below 1 in  $10 < E_{\text{Radiator}} < 20$  GeV and  $20 < E_{\text{Radiator}} < 30$  GeV. Comparing the values of the averaged splitting angles in  $D^0$  jets and in inclusive jets presented in Table. 1, we find the values in  $D^0$  jets are smaller than inclusive both in p+p and A+A in  $10 < E_{\text{Radiator}} < 20$  GeV and  $20 < E_{\text{Radiator}} < 30$  GeV. We find such puzzling results pointing to an important caveat.

We believe the number of splittings along the tracked prong in the investigated jets needs to be considered and further investigated. In the Table. 2, averaged splitting angles per splitting are calculated in  $D^0$ -meson (inclusive) jets in p+p and Pb+Pb at  $\sqrt{s} = 5.02$  TeV, besides that, the numbers of reconstructed splittings in jets are also provided accordingly. We find the averaged splitting angles per splitting of the  $D^0$ -meson jets are larger than that of the inclusive jets both in p+p and A+A, and the averaged splitting angles per splitting in A+A are also larger than their counterparts in p+p. We can also find the numbers of splittings in  $D^0$ -meson jets in each energy interval is always smaller than that in inclusive jets. All the calculations are cross-checked with LBT calculations [57, 58], The values of the calculation results in A+A collisions using LBT are 1 – 2% larger than that by using SHELL. Then the story of the dead-cone phenomenon affecting heavy flavor is

that the probability of heavy quark emitting gluon at a smaller angle is largely suppressed due to the dead-cone effect, leading it to be distributed at a larger angle. However, the possibility of emitting such gluon is suppressed due to this mass effect governed by the dead-cone term in Eq. 3.1.

## 5 Conclusions

We systematically calculate the emission angle distributions of charm-quark initiated splittings and that of light parton initiated splittings in p+p and Pb+Pb collisions at  $\sqrt{s} = 5.02$  TeV respectively. The same dead-cone effect is observed in p+p at  $\sqrt{s} = 5.02$  TeV as what ALICE reported at  $\sqrt{s} = 13$  TeV. The ratio of the number of jets normalized splitting angle distributions for  $D^0$ -meson jets and inclusive jets produced in Pb+Pb collisions  $R^{AA}(\theta)$  is predicted as a function of  $\ln(1/\theta)$  at different energy intervals. A suppression at the dead-cone region of  $\ln(1/\theta)$  is shown, indicating a direct observation of the dead-cone effect in medium-induced radiation. We also find the collisional energy loss mechanism will not compromise such observation. The averaged splitting angles per splittings for  $D^0$ -meson jets and inclusive jets in p+p and A+A are further calculated. We find the average splitting angle of the heavy flavor-initiated splitting is larger than that of the light flavor-initiated splitting and the number of splittings of the tracked prong in the heavy flavor-initiated jet is smaller than that in the inclusive jet. It indicates the dead-cone effect will lead to the survived splitting angle of heavy flavor-initiated splitting distributed at a larger angle, however, the possibility of such emission will be reduced.

## Acknowledgments

The authors would like to thank X Peng for helpful discussions. This research is supported by the Guangdong Major Project of Basic and Applied Basic Research No.2020B0301030008, the Natural Science Foundation of China with Project Nos. 11935007,12035007 and 11805167.

## References

- [1] S. Marzani, G. Soyez, and M. Spannowsky, Lecture Note in Physics **958**, 252 (2019).
- [2] Y. L. Dokshitzer, V. A. Khoze, and S. I. Troian, J. Phys. G **17**, 1602 (1991).
- [3] A. M. Sirunyan et al. (CMS), Phys. Rev. Lett. **125**, 102001 (2020), [1911.01461](#).
- [4] P. Abreu et al. (DELPHI), Phys. Lett. B **479**, 118 (2000), [Erratum: Phys.Lett.B 492, 398–398 (2000)], [hep-ex/0103022](#).
- [5] K. Abe et al. (SLD), Phys. Rev. Lett. **84**, 4300 (2000), [hep-ex/9912058](#).
- [6] J. Llorente and J. Cantero, Nucl. Phys. B **889**, 401 (2014), [1407.8001](#).
- [7] C. Frye, A. J. Larkoski, J. Thaler, and K. Zhou, JHEP **09**, 083 (2017), [1704.06266](#).
- [8] F. A. Dreyer, G. P. Salam, and G. Soyez, JHEP **12**, 064 (2018), [1807.04758](#).
- [9] P. Caucal, A. Soto-Ontoso, and A. Takacs, Phys. Rev. D **105**, 114046 (2022), [2111.14768](#).
- [10] P. Caucal, E. Iancu, and G. Soyez, JHEP **10**, 273 (2019), [1907.04866](#).

- [11] S. Acharya et al. (ALICE), *Nature* **605**, 440 (2022), [2106.05713](#).
- [12] X.-N. Wang and M. Gyulassy, *Phys. Rev. Lett.* **68**, 1480 (1992).
- [13] M. Gyulassy, I. Vitev, X.-N. Wang, and B.-W. Zhang, pp. 123–191 (2004), [nucl-th/0302077](#).
- [14] G.-Y. Qin and X.-N. Wang, *Int. J. Mod. Phys. E* **24**, 1530014 (2015), [1511.00790](#).
- [15] X.-f. Guo and X.-N. Wang, *Phys. Rev. Lett.* **85**, 3591 (2000), [hep-ph/0005044](#).
- [16] B.-W. Zhang and X.-N. Wang, *Nucl. Phys. A* **720**, 429 (2003), [hep-ph/0301195](#).
- [17] B.-W. Zhang, E. Wang, and X.-N. Wang, *Phys. Rev. Lett.* **93**, 072301 (2004), [nucl-th/0309040](#).
- [18] A. Majumder, *Phys. Rev. D* **85**, 014023 (2012), [0912.2987](#).
- [19] X.-F. Chen, C. Greiner, E. Wang, X.-N. Wang, and Z. Xu, *Phys. Rev. C* **81**, 064908 (2010), [1002.1165](#).
- [20] X.-F. Chen, T. Hirano, E. Wang, X.-N. Wang, and H. Zhang, *Phys. Rev. C* **84**, 034902 (2011), [1102.5614](#).
- [21] I. Vitev, M. Gyulassy, and P. Levai, *Acta Phys. Hung. A* **17**, 237 (2003), [nucl-th/0204019](#).
- [22] P. B. Arnold, G. D. Moore, and L. G. Yaffe, *JHEP* **11**, 001 (2000), [hep-ph/0010177](#).
- [23] P. B. Arnold, G. D. Moore, and L. G. Yaffe, *JHEP* **05**, 051 (2003), [hep-ph/0302165](#).
- [24] R. Baier, D. Schiff, and B. G. Zakharov, *Ann. Rev. Nucl. Part. Sci.* **50**, 37 (2000), [hep-ph/0002198](#).
- [25] Y. L. Dokshitzer and D. E. Kharzeev, *Phys. Lett. B* **519**, 199 (2001), [hep-ph/0106202](#).
- [26] N. Armesto, C. A. Salgado, and U. A. Wiedemann, *Phys. Rev. D* **69**, 114003 (2004), [hep-ph/0312106](#).
- [27] B.-W. Zhang, E.-k. Wang, and X.-N. Wang, *Nucl. Phys. A* **757**, 493 (2005), [hep-ph/0412060](#).
- [28] S. S. Adler et al. (PHENIX), *Phys. Rev. Lett.* **94**, 082301 (2005), [nucl-ex/0409028](#).
- [29] B. I. Abelev et al. (STAR), *Phys. Rev. Lett.* **98**, 192301 (2007), [Erratum: *Phys.Rev.Lett.* 106, 159902 (2011)], [nucl-ex/0607012](#).
- [30] B. Abelev et al. (ALICE), *JHEP* **09**, 112 (2012), [1203.2160](#).
- [31] V. Khachatryan et al. (CMS), *Eur. Phys. J. C* **77**, 252 (2017), [1610.00613](#).
- [32] ATLAS (ATLAS) (2022), [2204.13530](#).
- [33] T. Sjostrand, S. Mrenna, and P. Z. Skands, *Comput. Phys. Commun.* **178**, 852 (2008), [0710.3820](#).
- [34] M. Cacciari, G. P. Salam, and G. Soyez, *JHEP* **04**, 063 (2008), [0802.1189](#).
- [35] M. Cacciari, G. P. Salam, and G. Soyez, *Eur. Phys. J. C* **72**, 1896 (2012), [1111.6097](#).
- [36] Y. L. Dokshitzer, G. Leder, S. Moretti, and B. Webber, *JHEP* **08**, 001 (1997), [hep-ph/9707323](#).
- [37] A. Lifson, G. P. Salam, and G. Soyez, *JHEP* **10**, 170 (2020), [2007.06578](#).
- [38] W.-t. Deng and X.-N. Wang, *Phys. Rev. C* **81**, 024902 (2010), [0910.3403](#).

- [39] W. Dai, S. Wang, S.-L. Zhang, B.-W. Zhang, and E. Wang, *Chin. Phys. C* **44**, 104105 (2020), [1806.06332](#).
- [40] S. Wang, W. Dai, B.-W. Zhang, and E. Wang, *Chin. Phys. C* **45**, 064105 (2021), [2012.13935](#).
- [41] S. Wang, W. Dai, J. Yan, B.-W. Zhang, and E. Wang, *Nucl. Phys. A* **1005**, 121787 (2021), [2001.11660](#).
- [42] S. Wang, W. Dai, B.-W. Zhang, and E. Wang (2020), [2005.07018](#).
- [43] S. Acharya et al. (ALICE), *JHEP* **05**, 061 (2022), [2107.11303](#).
- [44] S. Cao, G.-Y. Qin, and S. A. Bass, *Phys. Rev. C* **88**, 044907 (2013), [1308.0617](#).
- [45] S. Wang, W. Dai, B.-W. Zhang, and E. Wang, *Eur. Phys. J. C* **79**, 789 (2019), [1906.01499](#).
- [46] M. He, H. van Hees, P. B. Gossiaux, R. J. Fries, and R. Rapp, *Phys. Rev. E* **88**, 032138 (2013), [1305.1425](#).
- [47] L. Pang, Q. Wang, and X.-N. Wang, *Phys. Rev. C* **86**, 024911 (2012), [1205.5019](#).
- [48] M. L. Miller, K. Reygers, S. J. Sanders, and P. Steinberg, *Ann. Rev. Nucl. Part. Sci.* **57**, 205 (2007), [nucl-ex/0701025](#).
- [49] G.-Y. Ma, W. Dai, B.-W. Zhang, and E.-K. Wang, *Eur. Phys. J. C* **79**, 518 (2019), [1812.02033](#).
- [50] Q. Zhang, W. Dai, L. Wang, B.-W. Zhang, and E. Wang (2022), [2203.10742](#).
- [51] L. Adamczyk et al. (STAR), *Phys. Rev. Lett.* **113**, 142301 (2014), [Erratum: *Phys.Rev.Lett.* 121, 229901 (2018)], [1404.6185](#).
- [52] G. Xie (STAR), *Nucl. Phys. A* **956**, 473 (2016), [1601.00695](#).
- [53] A. M. Sirunyan et al. (CMS), *Phys. Lett. B* **782**, 474 (2018), [1708.04962](#).
- [54] S. Acharya et al. (ALICE), *JHEP* **10**, 174 (2018), [1804.09083](#).
- [55] A. Francis, O. Kaczmarek, M. Laine, T. Neuhaus, and H. Ohno, *Phys. Rev. D* **92**, 116003 (2015), [1508.04543](#).
- [56] N. Brambilla, V. Leino, P. Petreczky, and A. Vairo, *Phys. Rev. D* **102**, 074503 (2020), [2007.10078](#).
- [57] Y. He, T. Luo, X.-N. Wang, and Y. Zhu, *Phys. Rev. C* **91**, 054908 (2015), [Erratum: *Phys.Rev.C* 97, 019902 (2018)], [1503.03313](#).
- [58] S. Cao, T. Luo, G.-Y. Qin, and X.-N. Wang, *Phys. Rev. C* **94**, 014909 (2016), [1605.06447](#).